TECHNICAL RESEARCH REPORT

SYSTEMS RESEARCH CENTER

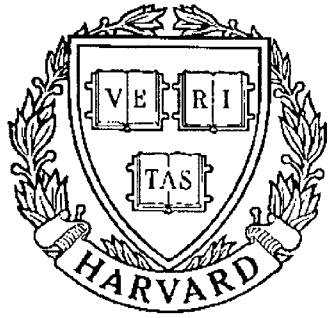

Supported by the National Science Foundation Engineering Research Center Program (NSFD CD 8803012), Industry and the University

Simulation of Intermittent Turning Processes

by G.M. Zhang, S. Yerramareddy, S.M. Lee, and S.C-Y. Lu

TR 89-91

Simulation of Intermittent Turning Processes

G. M. Zhang
Department of Mechanical Engineering and Systems Research Center
University of Maryland
College Park, MD 20742

S. Yerramareddy, S. M. Lee, and S. C-Y. Lu
Knowledge-Based Engineering Systems Research Laboratory
Department of Mechanical and Industrial Engineering
University of Illinois at Urbana-Champaign
1206 West Green Street
Urbana, IL 61801

Abstract

A simulation model is developed to study the dynamic characteristics of intermittent turning operations. Factors such as chip load, free-vibration of the toolpost structure, and nonhomogeneous hardness distribution in the material being cut are incorporated in the model. The principle of superposition is used in the formulation of the simulation algorithm. The impact between the cutting tool and the workpiece at the start of every cutting period during machining is treated as an initial value problem. The simulation model provides a quantitative evaluation of the tool vibratory motion during the intermittent turning process. Study of the cutting dynamics based on the simulation results not only confirms the experimental findings, but also indicates that increasing the static stiffness of the toolpost structure is an effective approach to control the tool vibratory motion. The determination of probability of tool breakage under various spindle speed settings is presented as an example to demonstrate the practical applications of the simulation model developed in this work.

1. Introduction

Due to the increasing demand for quality products, manufacturing engineers are faced with a difficult problem of increasing productivity without compromising quality. This problem is aggravated by the unique geometrical features demanded by the design engineers. Discontinuous geometries such as holes, key-ways, and slots that are located on the circumference of a workpiece pose such a problem in manufacturing. When these workpieces are being machined on a lathe, the cutting tool will not be engaged in cutting when it passes over the discontinuities. During such intermittent turning processes, the free-vibration of the toolpost and/or the workpiece is unavoidable. This introduces significant changes in the cutting dynamics. First, the machining system can easily become unstable because the cutting tool is oscillating severely during machining. Second, there is an impact between the cutting edge and the workpiece every time the tool passes over the discontinuity and starts to engage in cutting again. This may result in poor surface finish, and may cause the cutting edge to break. The increased cutting speeds being used to increase productivity, aggravate these problems and necessitate proper planning and control of the intermittent turning processes.

Previous research on intermittent turning processes focused on the stability analysis and the premature failure of the cutting edge [1-8]. Tlusty and Ismail investigated the dynamics of intermittent cutting during slot milling [1,2]. Proceeding along similar lines, Kapoor et al. proposed a time-varying parameter model to study the cutting dynamics during intermittent machining [3]. Based on such models, stability charts have been constructed to aid in the proper selection of cutting parameters that maintain the stability of the machining process [3]. It has been recognized that tool failure in intermittent turning is mainly due to thermal cracking, mechanical fatigue and sudden impact, in addition to the inevitable tool wear [6]. Bhatia [4] studied premature tool failure caused by thermal cracking and mechanical fatigue. However, due to the

increased cutting speeds being used at present, the importance of thermal and mechanical fatigue is outweighed by the importance of failure due to sudden impact. This requires an understanding of the cutting dynamics of the intermittent turning process. The sudden tool failure during machining, however, makes it very difficult to undertake experimental studies of the cutting dynamics at high spindle speeds.

In this paper, we present a new method for the dynamic analysis of intermittent turning processes. A model of a stable turning process that accounts for the important factors such as chip load, free-vibration of the toolpost structure, and nonhomogeneous hardness distribution in the material being cut is developed. The tool vibratory motion is quantitatively evaluated through simulation. The effects of important factors, such as spindle speed, on the cutting dynamics are studied. This demonstrates the importance of increasing the static stiffness of the toolpost structure for vibration control during machining. Finally, the determination of probability of tool breakage as a function of spindle speed is presented as an example to show how the present work can be applied to practical problems.

2. Model Development

Mathematical models such as the one embodied by the Merritt block diagram shown in Fig. 1 have been developed for describing the dynamic characteristics of machining processes. In these models, the machining process is viewed as a control system consisting of three parts, namely the cutting process, the machine tool structure, and the two feedback paths (the primary and the regenerative feedback paths). The input to this model is the nominal chip load and the output is the tool vibratory motion. However, the time-invariant system parameters used in these traditional models cannot adequately describe the cutting dynamics of an intermittent turning process [3]. During an intermittent turning process shown in Fig. 2, the cutting tool is repeatedly subjected to different modes of vibratory motion. In the cutting

period, the tool is engaged with the workpiece. Due to the cutting force generated, the tool vibrates about its dynamic equilibrium position. In the non-cutting period, the cutting tool is not engaged with the workpiece, and so the tool vibrates in free-vibration mode. In order to represent the dynamic characteristics of the intermittent turning process, a mathematical model which consists of two sub-models is needed. One sub-model is used to describe the forced-vibration of tool during the cutting period. The other is used to describe the free-vibration of tool in the non-cutting period.

2.1 Basic Assumptions

In order to develop a mathematical model for a preliminary investigation of the intermittent turning process, the following assumptions are made.

1. The feed is large, so that the regenerative feedback path shown in Fig. 1 can be omitted from the chatter loop.
2. The rigidity of workpiece is much higher than that of the toolpost, so that the tool vibratory motion is governed solely by the toolpost structure.
3. The impact between the rotating workpiece and the vibrating tool is mainly due to the dynamic chip load variation at the start of every cutting period to allow a one-degree-of-freedom model to be developed.

These assumptions can later be relaxed to develop a comprehensive model.

2.2 Basic Equations of Toolpost Structural Model

Tool vibratory motion is mainly caused by the cutting force generated during machining. Conventionally, the cutting force is evaluated as a function of chip load, which represents the cutting area during machining. The cutting area is expressed as a product of the width of cut and the thickness of cut, as shown in Fig. 2. The cutting

force can be assumed proportional to the chip load, where the proportionality coefficient K_a is called the unit cutting force [5].

$$\text{Nominal Cutting Force} = K_a \cdot \langle \text{Nominal Chip Load} \rangle = K_a \cdot w \cdot a(t) \qquad (1)$$

where w = width of cut = $d/\cos C_s$,

$a(t)$ = thickness of cut = $\begin{cases} a = f \cdot \cos C_s & \text{cutting period,} \\ 0 & \text{non-cutting period,} \end{cases}$

C_s = lead angle of tool,

d = depth of cut, and

f = feed.

The relation between the cutting force and the chip load given by Eq. (1) is valid only in the absence of tool vibration during machining. The chip load in Eq. (1) is, therefore, called the nominal chip load. Accordingly, the cutting force in Eq. (1) is called the nominal cutting force. However, the tool vibrates during machining. The tool vibratory motion in the direction normal to the machined surface, as indicated in Fig. 2, causes variation in the thickness of cut, leading to an instantaneous chip load variation. As a result, the instantaneous cutting force is given by

$$\text{Instantaneous Cutting Force} = K_a \cdot w \cdot [a(t) - y(t)] \qquad (2)$$

where $y(t)$ = magnitude of tool vibration in the direction normal to the machined surface.

In order to evaluate the tool vibratory motion in the direction normal to the machined surface, the toolpost structure on which the tool is firmly supported is

modeled as a second-order system shown in Fig. 3. For the cutting period, the mathematical form of this second-order structural model is given by

$$M\frac{d^2[y(t)]}{dt^2} + C\frac{d[y(t)]}{dt} + K[y(t)] = \{K_a \cdot w \cdot [a - y(t)]\} \cdot \cos\theta \qquad (3)$$

where M = lumped mass of the toolpost structure,

C = damping factor of the toolpost structure,

K = static stiffness of the toolpost structure, and

θ = projection angle of the cutting force with respect to the direction normal to the machined surface.

For the non-cutting period, the mathematical form of the toolpost structural model is given by

$$M\frac{d^2[y(t)]}{dt^2} + C\frac{d[y(t)]}{dt} + K[y(t)] = 0 \qquad (4)$$

As can be seen from Eq. (4), there is no cutting force generation during the non-cutting period.

2.3 Identification of Initial Conditions

The evaluation of tool vibratory motion based on Eqs. (3) and (4) is related to the initial conditions of tool motion at the beginning of the cutting period and the non-cutting period, respectively. There are three distinct kinds of initial conditions.

1. At the beginning of the intermittent turning process,
   the tool is stationary at its preset position. Therefore, the initial displacement and velocity of the tool are equal to zero, i.e.,

$$y(t)|_{t=o} = 0 \quad \text{and} \quad \dot{y}(t)|_{t=0} = 0$$

2. At the beginning of the non-cutting period,
the tool is just through the cutting period. Therefore, the initial displacement and velocity of the tool used to evaluate the free-vibratory motion of the tool are determined by the forced-vibratory motion of the tool at the end of the cutting period, i.e.,

$$y_{free}(T_1 + 0) = y_{forced}(T_1) \quad \text{and}$$
$$\dot{y}_{free}(T_1 + 0) = \dot{y}_{forced}(T_1)$$

where T_1 represents the time duration of the cutting period.

3. At the beginning of the cutting period,
the tool is just through the non-cutting period. Therefore, the initial displacement and velocity of the tool used to evaluate the forced-vibratory motion of the tool are determined by the free-vibratory motion of the tool at the end of the non-cutting period, i.e.,

$$y_{forced}(T_2 + 0) = y_{free}(T_2) \quad \text{and}$$
$$\dot{y}_{forced}(T_2 + 0) = \dot{y}_{free}(T_2)$$

where T_2 represents the time duration of the non-cutting period.

2.4 Incorporation of Random Excitation

The forced- and the free-vibrations discussed above cannot completely describe the practically observed vibratory motion of the cutting tool during machining. There is

an additional random component which indicates that the cutting tool is subjected to random excitation during machining. Though there could be a number of other sources, the major source of random excitation can be attributed to the nonhomogeneous hardness distribution in the workpiece material being machined [9].

In order to incorporate the random excitation into the evaluation of tool vibratory motion, a stochastic model [11] that approximates the hardness variation as a normal distribution with mean (μ_a) and variance (σ_s^2), is used in the present work. The deviation of the cutting force from the nominal value is expressed as a random cutting force, which is given by [11]

$$\text{Random Cutting Force} = K_a \cdot w \cdot a \cdot \{[\frac{\mu_s(t)}{\mu_a}]^m - 1\} \qquad (5)$$

where $\mu_s(t)$ represents the hardness at the cutting location at any particular instant in time, t, and "m" is the Meyer exponent that explains the nonlinear relation between the cutting force and the hardness ration, $[\mu_s(t)/\mu_a]$. The Meyer exponent can be found in the metal cutting handbooks. For example, m = 0.454 for carbon steel and m = 0.418 for copper [10]. In the present work, a random number generator is used to simulate the hardness distribution.

2.5 Simulation Model

As discussed in the previous sections, Eqs. (3) and (4) represent the mathematical forms of the toolpost structural model for the cutting and the non-cutting periods, respectively. Equation (5) represents the component of the cutting force generated due to the random excitation caused by the nonhomogeneous hardness distribution in the workpiece material. Combining these three equations together with

the appropriate initial conditions, results in the simulation model used in the present work. It is given as follows.

Simulation Model =

Cutting Period:

$$M\frac{d^2[y(t)]}{dt^2} + C\frac{d[y(t)]}{dt} + K[y(t)] =$$

$$\{K_a \cdot w \cdot [a(t) - y(t)] + K_a \cdot w \cdot a \cdot [(\frac{\mu_s(t)}{\mu_a})^m - 1]\} \cos\theta$$

$$y(t)|_{t=o} = 0 \quad \text{and} \quad \dot{y}(t)|_{t=0} = 0 \text{ or}$$

$$y_{free}(T_1 + 0) = y_{forced}(T_1)$$

$$\dot{y}_{free}(T_1 + 0) = \dot{y}_{forced}(T_1)$$

Non-Cutting Period:

$$M\frac{d^2[y(t)]}{dt^2} + C\frac{d[y(t)]}{dt} + K[y(t)] = 0$$

$$y_{forced}(T_2 + 0) = y_{free}(T_2)$$

$$\dot{y}_{forced}(T_2 + 0) = \dot{y}_{free}(T_2)$$

The simulation model represented by Eq. (6) is a time-varying parameter model, as evidenced by the two natural frequencies associated with the model. The natural frequency changes alternatively from a higher value during the cutting period to a lower value during the non-cutting period. This system model decomposes the intermittent turning process into two sub-systems and applies initial conditions as a transient process between the cutting and the non-cutting periods. This makes it possible to treat the two sub-systems as time-invariant systems. As a result, analytical solutions to Eq. (6) can be derived with ease. They form a basis for developing a

computer program to study the dynamic characteristics of the intermittent turning process.

3. Numerical Simulation

There are several reasons for performing numerical simulation of the cutting dynamics of the intermittent turning process. First, the probability of tool breakage during machining is high, especially at high spindle speeds. This poses many difficulties in conducting experimental studies, not only in terms of increased cost but also introducing noise into the measured data, because of the necessity of using different tool inserts in a single test. Second, most dynamometers are designed for measuring cutting forces under continuous machining conditions, and hence are not suitable to monitor the cutting force under intermittent machining conditions.

The procedure developed in the present work to perform the numerical simulation consists of three major steps, namely, evaluation of the force function which is the input to the simulation model, derivation of the analytical solution forms for both the forced and the free vibratory motion, and evaluation of the tool vibratory motion under random excitation.

3.1 Force Function

As indicated in Fig. 3, the dynamic cutting force generated during machining consists of two parts. One part is contributed by the chip load and the other part is a result of the random excitation. As indicated in Eq. (2), the chip load at any instant during cutting is determined by the algebraic sum of the nominal chip load, $[w \cdot a]$, and the chip load variation through the primary feedback path, $[w \cdot y(t)]$. Values of the proportionality coefficient K_a, which is mainly determined by the material being machined, can be found in machining handbooks. For example, $K_a = 2.0 \times 10^9$ for machining 1040 steel [10].

As discussed in section 2, the random excitation during machining is mainly due to the nonhomogeneous hardness distribution in the material being machined. This distribution can be described by a normal distribution, which can be converted to its equivalent random cutting force using Eq. (5). A brief explanation of the procedure used to calculate the random cutting force is described next.

Each cutting period (T_1) is divided into a fixed number (N) of equal divisions, for example, 40. The hardness is assumed to be uniform over each division. The N hardness values would follow the normal distribution with mean μ_a and variance σ_s^2. This hardness distribution results in a series of random excitation forces at intervals of time given by

$$\text{Time Interval} = \Delta t = \frac{\text{Time Duration of Cutting Period (T1)}}{\text{Number of Cutting Locations (N)}} \tag{7}$$

The effects of the random excitation forces are incorporated into the simulation program by using the principle of superposition. Figure 4 shows the hardness distribution and the corresponding magnitudes of the random cutting force, used in the present work.

3.2 Form of Analytical Solutions

The simulation algorithm developed in the present work is based on the analytical solutions to the simulation model given by Eq. (6). Let us define the circular natural frequency of the toolpost structure, which dominates the tool vibration during the non-cutting period, by the term

$$\omega_{n2} = \sqrt{\frac{K}{M}} \tag{8}$$

The circular natural frequency of the intermittent turning system, which dominates the tool vibration during the cutting period, is given by

$$\omega_{n1} = \sqrt{\frac{K + K_a \cdot w \cdot \cos\theta}{M}} \tag{9}$$

Comparing the two frequencies, we observe that the frequency associated with the intermittent turning system is higher than that associated with the toolpost structure.

As discussed earlier, the time-varying parameter model can be treated as two time-invariant sub-models, one each for the cutting period and the non-cutting period. The analytical solution to the time-invariant sub-models can be derived as follows, based on the corresponding initial conditions.

1. Normalizing Eq. (6) by the factor 1/M and introducing the following notation,

$$\frac{C}{M} = 2\zeta_1\omega_{n1} = 2\zeta_2\omega_{n2} \tag{10}$$

where ζ_1 and ζ_2 are damping coefficients of the toolpost structure and the intermittent turning system, respectively, and

$$\frac{K_a \cdot w \cdot a \cdot \sin\theta}{M} \cdot \left[\frac{\mu_s(t)}{\mu_a}\right]^m = \frac{1}{\omega_n^2} \cdot \frac{K_a \cdot w \cdot a \cdot \cos\theta}{K} \cdot \left[\frac{\mu_s(t)}{\mu_a}\right]^m$$

$$= \frac{K_m}{\omega_n^2} \cdot \left[\frac{\mu_s(t)}{\mu_a}\right]^m \tag{11}$$

where K_m is defined as $\frac{K_a \cdot w \cdot a \cdot \cos\theta}{K}$, which is a magnification factor.

2. Taking Laplace transformation of Eq. (6) to derive the analytical solution of the tool vibratory motion in the Laplace domain, which is given by

$$Y(s) = Y_1(s) + Y_2(s) + Y_3(s)$$

$$= K_m \cdot \frac{\omega_n^2}{s[(s + \zeta\omega_n)^2 + (\omega_n \sqrt{1 - \zeta^2})^2]}$$

$$+ [2\zeta\omega_n y(0) + \dot{y}(0)] \left[\frac{1}{(s + \zeta\omega_n)^2 + (\omega_n \sqrt{1 - \zeta^2})^2}\right]$$

$$+ \frac{sy(0)}{(s + \zeta\omega_n)^2 + (\omega_n \sqrt{1 - \zeta^2})^2} \qquad (12)$$

3. Derive the analytical solutions in the time domain by taking the inverse Laplace transformation and applying the initial conditions where appropriate,

$$y(t) = y_1(t) + y_2(t) + y_3(t)$$

$$= K_m \cdot \{1 + \frac{1}{1 - \sqrt{1 - \zeta^2}} e^{-\zeta\omega_n t} \sin(\omega_n \sqrt{1 - \zeta^2} t - \arctan \frac{\sqrt{1 - \zeta^2}}{-\zeta})\}$$

$$+ \{\frac{2\zeta\omega_n y(0) + \dot{y}(0)}{\omega_{n2}\sqrt{1 - \zeta^2}} e^{-\zeta\omega_n t} \sin (\omega_n \sqrt{1 - \zeta^2} t)\}$$

$$+ \{\frac{y(0)}{\sqrt{1 - \zeta^2}} e^{-\zeta\omega_n t} \sin (\omega_n \sqrt{1 - \zeta^2} t + \arctan \frac{\sqrt{1 - \zeta^2}}{-\zeta})\} \qquad (13)$$

3.2.1 Analytical Solution of Forced-Vibration without Random Excitation

During the cutting period, there are two types of initial conditions. At the beginning of machining, all the initial conditions are zero. Therefore, the analytical solution consists of only one term of Eq. (13), $y_1(t)$. It is given by

$$y(t) = y_1(t)$$

$$= K_m \cdot \{1 + \frac{1}{1 - \sqrt{1 - \zeta_1}} e^{-\zeta_1 \omega_{n1} t} \sin(\omega_{n1} \sqrt{1 - \zeta_1^2} t - \arctan \frac{\sqrt{1 - \zeta_1^2}}{-\zeta_1})\} \quad (14)$$

During machining, the initial conditions are, in most cases, nonzero. The analytical solution consists of the three terms of Eq. (13). It is given by

$$y(t) = y_1(t) + y_2(t) + y_3(t)$$

$$= K_m \cdot \{1 + \frac{1}{1 - \sqrt{1 - \zeta_1^2}} e^{-\zeta_1 \omega_{n1} t} \sin(\omega_{n1} \sqrt{1 - \zeta_1^2} t - \arctan \frac{\sqrt{1 - \zeta_1^2}}{-\zeta_1})\}$$

$$+ \{\frac{2\zeta_1 \omega_{n1} y(0) + \dot{y}(0)}{\omega_{n1} \sqrt{1 - \zeta_1}} e^{-\zeta_1 \omega_{n1} t} \sin(\omega_{n1} \sqrt{1 - \zeta_1^2} t)\}$$

$$+ \{\frac{y(0)}{\sqrt{1 - \zeta_1^2}} e^{-\zeta_1 \omega_{n1} t} \sin(\omega_{n1} \sqrt{1 - \zeta_1^2} t + \arctan \frac{\sqrt{1 - \zeta_1^2}}{-\zeta_1})\} \quad (15)$$

3.2.2 Analytical Solution of Free-Vibration

During the non-cutting period, the initial conditions are not zero, but the cutting force becomes zero. Therefore, the analytical solution consists of two terms of Eq. (13), i.e., $y_2(t)$ and $y_3(t)$. It is given by

$$y(t) = y_2(t) + y_3(t)$$

$$+ \{\frac{2\zeta_2\omega_{n2}y(0) + \dot{y}(0)}{\omega_{n2}\sqrt{1 - \zeta_2^2}} e^{-\zeta_2\omega_{n2}t} \sin(\omega_{n2}\sqrt{1 - \zeta_2^2}t)\}$$

$$+ \{\frac{y(0)}{\sqrt{1 - \zeta_2^2}} e^{-\zeta_2\omega_{n2}t} \sin(\omega_{n2}\sqrt{1 - \zeta_2^2}t + \arctan\frac{\sqrt{1 - \zeta_1^2}}{-\zeta_2})\} \qquad (16)$$

3.2.3 Analytical Solution of Forced-Vibration with Random Excitation

As indicated in Fig. 3, the toolpost structural model is also subjected to the random excitation, in addition to the cutting force contributed by the chip load. Because the simulation model developed in the present work is a linear system, the principle of superposition is valid. Therefore, an additional term, which is contributed by the random excitation, should be added to the analytical solution given by Eq. (15) (note: Eq. (14) for the first cutting period). The additional term can be expressed in the following form.

$$y_a(t') = \sum_{i=1}^{t'/\Delta t} \{[\frac{\mu_s(i\Delta t)}{\mu_a}]^m - [\frac{\mu_s((i-1)\Delta t)}{\mu_a}]^m\} \cdot$$

$$K_m \cdot \{(1 + \frac{1}{\sqrt{1 - \zeta_1^2}} e^{-\zeta_1\omega_{n1}t'} \sin(\omega_{n1}\sqrt{1 - \zeta_1^2}t' - \arctan\frac{\sqrt{1 - \zeta_1^2}}{-\zeta_1})\} \qquad (17)$$

where t' ($0 \le t' \le T_1$) represents the time counted from the beginning of each cutting period.

3.3 Cast Studies

To study the cutting dynamics of the intermittent turning process, computer simulations were carried out using the parameter settings listed below. They were based on the data provided in [10] and the experimental results presented in [3].

For the machine tool:

static stiffness $K = 1.0 \times 10^6$ N/m

equivalent mass M = 0.7 kg.

damping factor C = 140 rad/sec.

For the workpiece:

material = 1040 steel.

unit cutting force $K_a = 2.0 \times 10^9$ N/m^2.

mean of hardness distribution $\mu_a = 175$ (BHN).

variance of hardness distribution $\sigma_s^2 = 172$ (BHN)^2.

Meyer exponent m = 0.454.

geometry (Table 1)

diameter = 100 mm

number of slots = 2

width of slot = 60 mm

For the cutting tool:

lead angle Cs = 30 degrees.

In the present work, six case studies are conducted. The simulation conditions are listed in Table 1. In Case 1 and Case 6, the simulation of the tool vibratory motion

is based on a continuous turning process, without and with the presence of random excitation, respectively. In Case 2, the simulation of the tool vibration motion is based on a discontinuous turning process without the presence of random excitation. A 1040 carbon steel workpiece having two even spacings on its circumference (Table 1) is assumed. The simulation conditions used in Case 4 are similar to those used in Case 2 except that random excitation is present in Case 4. The only difference in the simulation conditions among Cases 3, 4, and 5 is the spindle speed. It is set at 300 rpm in Case 3, 600 rpm in Case 4, and 1200 rpm in Case 5.

4 Discussion of Results

4.1 Characteristics of Tool Vibratory Motion

The simulated tool vibratory motion during a continuous turning process is shown in Fig. 5a. The tool vibratory motion is significant only at the beginning of the cutting process due to the sudden application of the nominal chip load. Since random excitation is not considered during simulation, the tool vibratory motion attenuates due to the damping effect. Figure 5b depicts the simulated tool vibratory motion during an intermittent turning process. The tool vibration is significant throughout the machining process. Comparing the two cases, it is evident that the repeated sudden application of the nominal chip load and the free-vibration of the tool during the non-cutting period play an important role in increasing the vibratory motion during an intermittent turning process.

4.2 Importance of Incorporating the Random Excitation

The difference between the simulated results shown in Fig. 5b and Fig. 5d represents the effect of the random excitation on the tool vibratory motion during the cutting period. A careful examination of the two simulated results reveals that the vibration pattern shown in Fig. 5b is solely deterministic, and that the vibration pattern

shown in Fig. 5d consists of both deterministic and random components. More important is the fact that there is a constant level of residual tool vibration in Fig. 5d. The vibratory motion shown in Fig. 5d resembles more closely the tool vibratory motion normally observed in practice. Figure 5f gives the simulated tool vibratory motion during a continuous turning process with random excitation. This also shows the constant level of residual tool vibration, once again confirming the importance of the random excitation.

4.3 Effect of Spindle Speed on Tool Vibratory Motion

As indicated in Eq. (15), the tool vibratory motion is composed of three parts, i.e., $y_1(t)$, $y_2(t)$, and $y_3(t)$. The magnitude of $y_1(t)$ is related to the nominal chip load, and the magnitude of $y_2(t)$ is mainly related to the tool initial velocity, and the magnitude of $y_3(t)$ is related to the tool initial displacement at the start of a cutting period.

As illustrated in Fig. 5, the initial displacement and velocity of tool at the start of a cutting period are determined by the free-vibration of the tool at the end of the non-cutting period. Hence, the time duration of the non-cutting period is a critical factor in determining the tool vibratory motion during the cutting period. For the workpiece geometry (Fig. 2 and Table 1) used in the simulation, the time duration of the non-cutting period is given by

$$T2 = \left[\frac{60}{\text{Spindle Speed}}\right]\left[\frac{\arcsin \frac{\text{Width of Slot}}{\text{Diameter}}}{\pi}\right] \cdot 2 \qquad (18)$$

where two diametrically opposite slots are assumed.

According to Eq. (18), the time durations of the non-cutting period in Cases 3, 4, and 5 are 0.04 sec, 0.02 sec, and 0.01 sec, respectively. In order to quantitatively compare the tool vibratory motion at different spindle speeds, an index - the mean of

the maximum overshoot of the tool vibration during cutting periods is used. As indicated in Figs. 5c, 5d, and 5e, the means of the maximum overshoot of the tool vibratory motion during the cutting period in the three cases are 68 μm, 88 μm, and 104 μm, respectively. It is evident that the mean value increases as the spindle speed increases. Table 2 lists 11 such means where each mean is an average of 10 individual values of maximum overshoot based on the simulation results. Table 2 also lists the corresponding standard deviation values to indicate the variation level of maximum overshoot about its mean. Figure 6 is a plot of the relation between the mean level of maximum overshoot and the time duration of the non-cutting period presented in Table 3. Two observations can be made after a careful examination of Fig. 1.

1. The shorter the time duration of the non-cutting period or the higher the spindle speed, the larger the mean level of maximum overshoot. For example, the mean level of maximum overshoot is 12 μm at a spindle speed of 200 rpm, but 104 μm at a spindle speed of 1200 rpm.

2. The mean level of maximum overshoot fluctuates in high spindle speed regions. For example, the mean level reaches its first peak at a spindle speed of 400 rpm, but drops as the spindle speed increases. The mean level goes up again when the spindle speed is above 800 rpm, and reaches a second peak at a spindle speed of 900 rpm.

The simulated data presented in Table 3 provide an insight into how the spindle speed affects the status of tool vibration at the end of the non-cutting period, which in turn affects the tool vibration during the cutting period. The data for the spindle speed of 1200 rpm indicates that the maximum variation ranges of $y_1(t)$, $y_2(t)$, and $y_3(t)$ are

185 μm, 74 μm, and 28 μm, respectively. Therefore, they account for 64%, 26%, and 10% of the total displacement variation range during the cutting period. This indicates that the initial velocity plays a relatively important role (26%) in determining the maximum variation range at a high spindle speed setting. Similarly, examining the data for the spindle speed of 600 rpm, the corresponding percentages are 85%, 8%, and 7%, respectively. This indicates that the influence exerted by either the initial displacement or the initial velocity decreases as the spindle speed decreases. This suggests that as the spindle speed increases, the initial velocity increases dramatically, thereby increasing the mean levels of maximum overshoot of the total vibration during the cutting periods, leading to a significant variation of the chip load during machining.

From Eq. (15), it is clear that the magnitude of $y_2(t)$ is inversely proportional to the circular natural frequency of the intermittent turning system, ω_{n2}. This indicates that the most effective way to reduce the magnitude of $y_2(t)$ for a given initial velocity is to increase the value of ω_{n2}. This requires an increase in the static stiffness of the toolpost structure, K.

The fluctuation of the mean of maximum overshoot at high spindle speed ranges is due to the wide variation in the initial displacement/velocity about the zero (node position) at the start of the cutting period. This fluctuation is in agreement with the experimental findings in [3]. It also supports the heuristic knowledge of experienced operators on the shop-floor, who often change the spindle speed a little higher to control the tool vibration.

4.4 Application of Simulation Results

One practical application of the present work is to provide a reasonable method to establish the probability of tool breakage during the intermittent turning process. It has been observed on the shop floor that the tool breakage during the intermittent

turning process occurs very often. The major causes could be thermal cracking, mechanical fatigue, and sudden impact between the rotating workpiece and the vibrating tool [4-6]. However, at high spindle speed ranges, the sudden impact becomes the dominant factor causing the tool cutting edge failure. If the impact is mainly due to the dynamic variation of the chip load, the present work offers a way to assess the probability of tool breakage during machining. In Table 2, the mean and standard deviation of the maximum overshoots of the tool vibration are given and can be used to measure the dynamic variation of the chip load. It can be safely assumed that tool breakage occurs if the maximum overshoot exceeds a certain limiting value. This limiting value, of course, depends on the tool and workpiece materials. In the present work, a limiting value of 100 μm is assumed based on tool breakage data obtained from limited experimentation. The probabilities of tool breakage at different spindle speeds can be determined based on either a t-distribution or a normal distribution. For example, the mean and standard deviation of maximum overshoot are 12 and 4.57 μm, respectively, at a spindle speed of 200 rpm, as indicated in Table 2. The probability of tool breakage would be zero based on a normal distribution. At a spindle speed of 600 rpm, the probability would be 17% based on a normal distribution, $N[88, (12.5)^2]$. Such a probability would be 63% at a spindle speed of 1200 rpm based on $N[104, (12.4)^2]$. These probabilities can be effectively used for reasoning under uncertainty, in an expert system.

5. Conclusions

1. A simulation model is developed to study the dynamic characteristics of the intermittent turning process. The model decomposes the intermittent machining process into two sub-models, one each for the cutting and the non-cutting periods. The tool vibratory motion at the end of each period serves as the initial condition that determines the tool vibratory motion during the succeeding period.

An analytical solution for each period is derived and incorporated into a computer program to simulate the tool vibratory motion during the intermittent turning process.

2. Random excitation, based on the nonhomogeneous hardness distribution in the workpiece material, is incorporated into the system model to explain the random vibratory motion of the tool. The principle of superposition is employed to add together the effects of the random excitation and the nominal chip load.
3. The simulation results vividly depict the effect of free-vibration of the tool on the tool vibration during the cutting period. Thus, the time duration of the non-cutting period is a critical factor in determining the tool vibratory motion. A preliminary investigation of the relation between the mean levels of the maximum overshoot of the tool vibratory motion and the spindle speed indicates that high initial velocity at the start of the cutting period results in a high mean level of maximum overshoot. An effective way to control the maximum overshoot is to increase the static stiffness of the toolpost structure.
4. The determination of probability of tool breakage based on the simulation results is shown as an example of the practical applications of this work. The derived probabilities could be used for reasoning under uncertainty in an expert system.

Acknowledgments

The authors acknowledge the support of the Systems Research Center at the University of Maryland at College Park under Engineering Research Centers Program: NSFD CDF 8803012. Part of the funding for this research is provided by the Digital Equipment Corporation and the University of Illinois Research Board.

References

1. J. Tlusty and F. Ismail, "Basic Non-Linearity in Machining Chatter," Annals of the CIRP, Volume 30/1/1981, pp. 299-304.
2. J. Tlusty and F. Ismail, "Special Aspects of Chatter in Milling," Journal of Vibration, Acoustics, Stress, and Reliability in Design, Trans. ASME, Volume 105, 1983, pp. 24-32.
3. S. G. Kapoor, F. Ding, G. M. Zhang, and R. E. DeVor, "A Time-Varying Parameter Model for the Stability Analysis of Intermittent Turning Process," Proceedings of the 13th North American Manufacturing Research Conference, May 1985, pp. 551-557.
4. S. M. Bhatia, P. C. Pandey, and H. S. Shah, "Failure of Cemented Carbide Tools When Executing Intermittent Cuts," Journal of Engineering for Industry, Trans. ASME, Volume 101, November 1979, pp. 391-396.
5. N. N. Zorev, "Machining Steel with a Carbide Tipped Tool in Interrupted Heavy Cutting Conditions," Russian Engineering Journal, Volume 43, No. 2, 1963, p. 43.

6. G. S. Andreev, "Thermal State of Tool Cutting Edge in Intermittent Metal Cutting," Russian Engineering Journal, Volume 54, No. 8, 1974, p. 56.
7. Z. Palmar, "Cutting Temperature in Intermittent Cutting," International Journal of Machine Tools and Manufacturing, Volume 27, No. 2, 1987, pp. 261-274.
8. N. N. Zerov and H. A. Sawaiaskin, "Carbide Cutting Tool Life at Interrupted Cut with Continuous Cycles," Annals of the CIRP, Volume 18, 1970, p. 555.
9. M. E. Merritt, "Theory of Self-Excited Machine-Tool Chatter," Journal of Engineering for Industry, Trans. ASME, Volume 87, November 1965, pp. 447-454.
10. M. Kronenberg, Machining Science and Application, Pergamon Press, Inc., 1966.
11. G. M. Zhang, "Dynamic Modeling and Dynamic Analysis of the Boring Machining System," Ph.D. Thesis, University of Illinois at Urbana-Champaign, U.S.A., January 1986.

NOMENCLATURE

a	=	thickness of cut during the cutting period
a(t)	=	thickness of cut during the entire intermittent turning process
BHN	=	Brinell hardness number
C	=	damping factor used in the toolpost structural model
C_s	=	lead angle of tool
d	=	depth of cut, cutting parameter
f	=	feed, cutting parameter
i	=	an index
K	=	static stiffness of the toolpost structure
K_a	=	unit cutting force
K_m	=	magnification factor
M	=	equivalent mass of the toolpost structure
m	=	Meyer exponent used to evaluate the random part of cutting force
N	=	number of divisions along the circumference of workpiece
s	=	complex variable used in the Laplace transformation, or the width of slot on the circumference of workpiece
T_1	=	time duration of the cutting period
T_2	=	time duration of the non-cuting period
t	=	time evaluated from the beginning of the entire intermittent turning process
t'	=	time evaluated from the beginning of the cutting period
w	=	width of cut
y(t)	=	displacement of tool vibratory motion in the direction normal to the machined surface
$y_{free}(t)$	=	displacement of tool vibratory motion in the direction normal to the machined surface during the non-cutting period

$y_{forced}(t)$ = displacement of tool vibratory motion in the direction normal to the machined surface during the cutting period

$y_1(t)$ = part of the displacement of tool vibratory motion contributed by the nominal chip load

$y_2(t)$ = part of the displacement of tool vibratory motion mainly contributed by the initial velocity

$y_3(t)$ = part of the displacement of tool vibratory motion contributed by the initial displacement

$y_a(t')$ = part of the displacement of tool vibratory motion contributed by the random excitation

$\dot{y}(t)$ = velocity of tool vibratory motion in the direction normal to the machined surface

$\dot{y}_{free}(t)$ = velocity of tool vibratory motion in the direction normal to the machined surface during the non-cutting period

$\dot{y}_{forced}(t)$ = velocity of tool vibratory motion in the direction normal to the machined surface during the cutting period

Δt = uniform time interval used in simulation

μ_a = mean of hardness distribution

μ_s = hardness value at individual cutting locations

ω_{n1} = natural circular frequency of intermittent turning system

ω_{n2} = natural circular frequency of toolpost structure

σ_s^2 = variance of hardness distribution

ζ_1 = damping coefficient of intermittent turning system

ζ_2 = damping coefficient of toolpost structure

List of Figures

Fig. 1 Merrit Block Diagram Representing the Machining Process

Fig. 2 Intermittent Turning Process

Fig. 3 Structure of the Intermittent Turning Process Model

Fig. 4 Evaluation of the Random Excitation Force

Fig. 5 Simulation Results of the Six Case Studies

Fig. 6 Relation between the Mean of Maximum Overshoot and Spindle Speed

List of Tables

Table 1 Simulation Conditions Used in the Case Studies

Table 2 Calculation of the Mean of Maximum Overshoot as a Function of the Spindle Speed

Table 3 Decomposition of the Tool Vibration during the Cutting Period

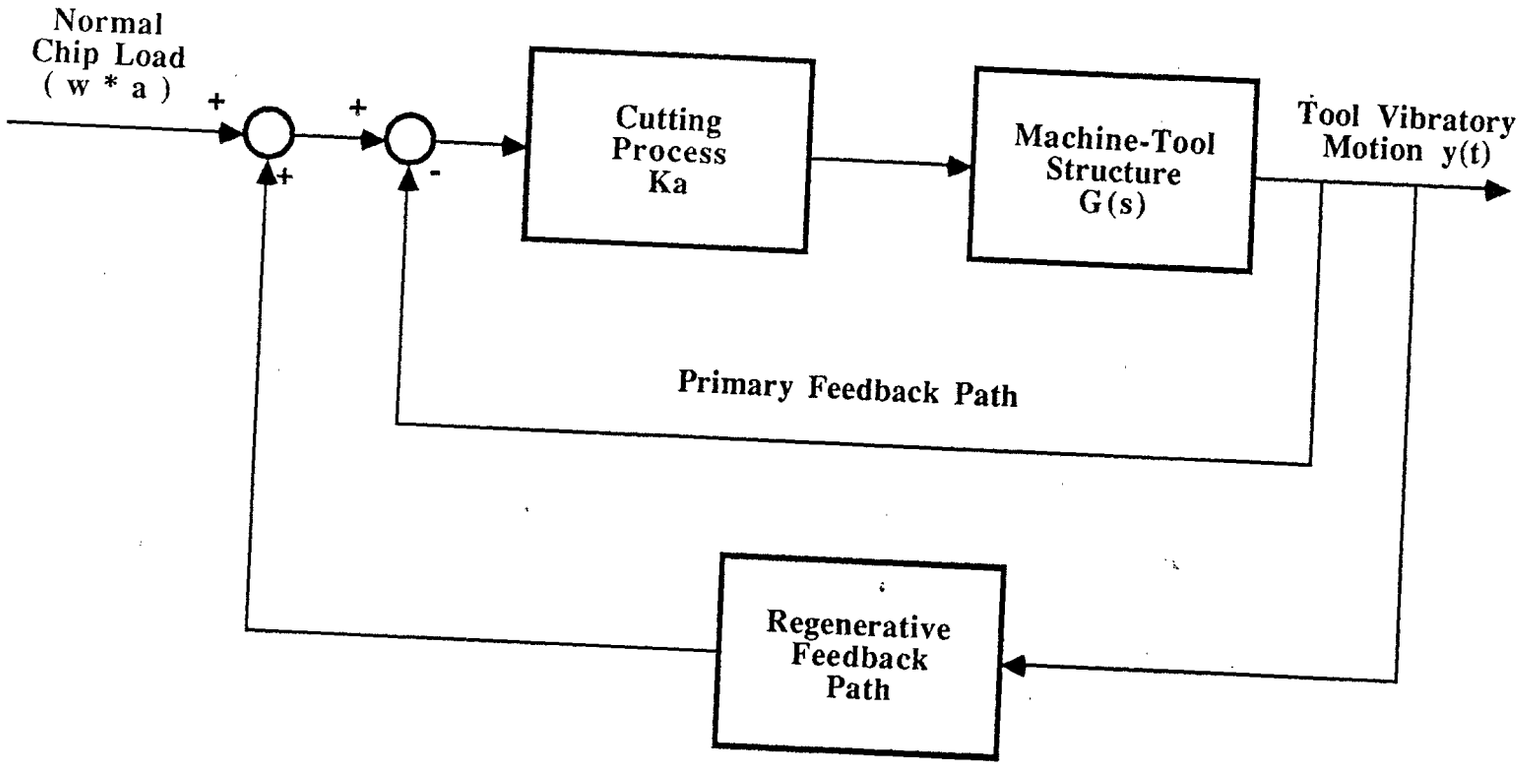

Fig. 1 Merritt Block Diagram Representing the Machining Process

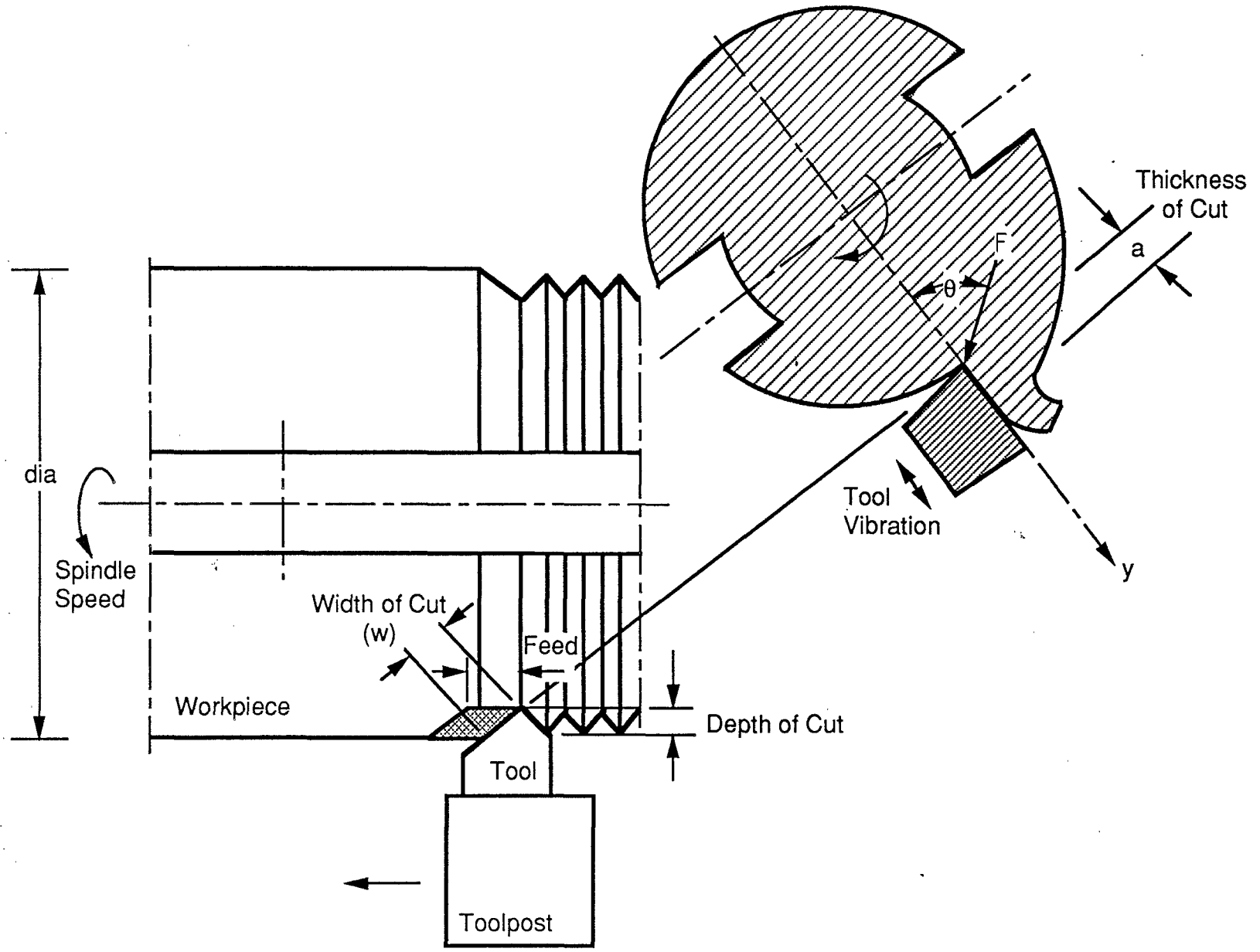

Fig. 2 Intermittent Turning Process

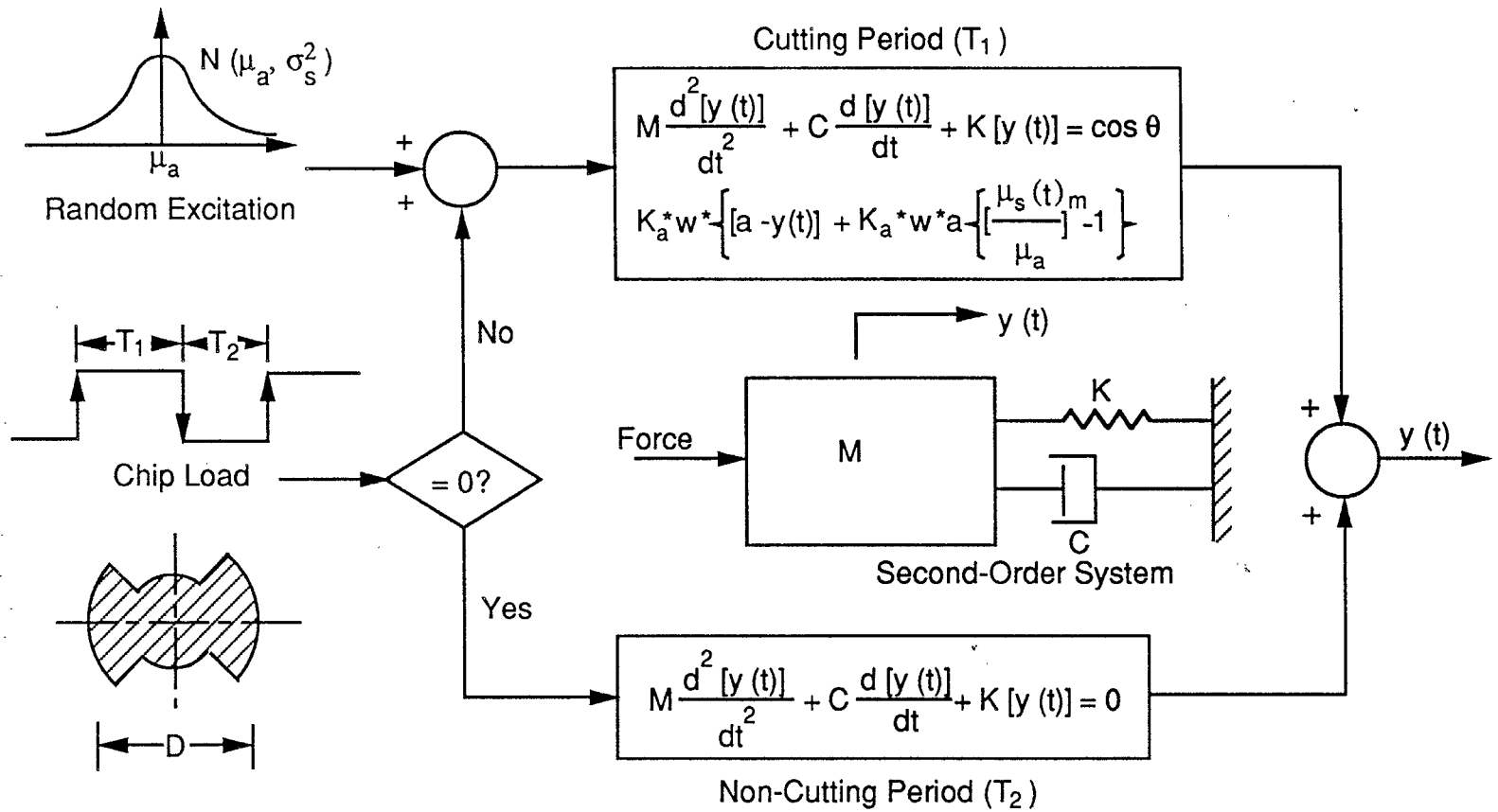

Fig. 3 Structure of the Intermittent Turning Process Model

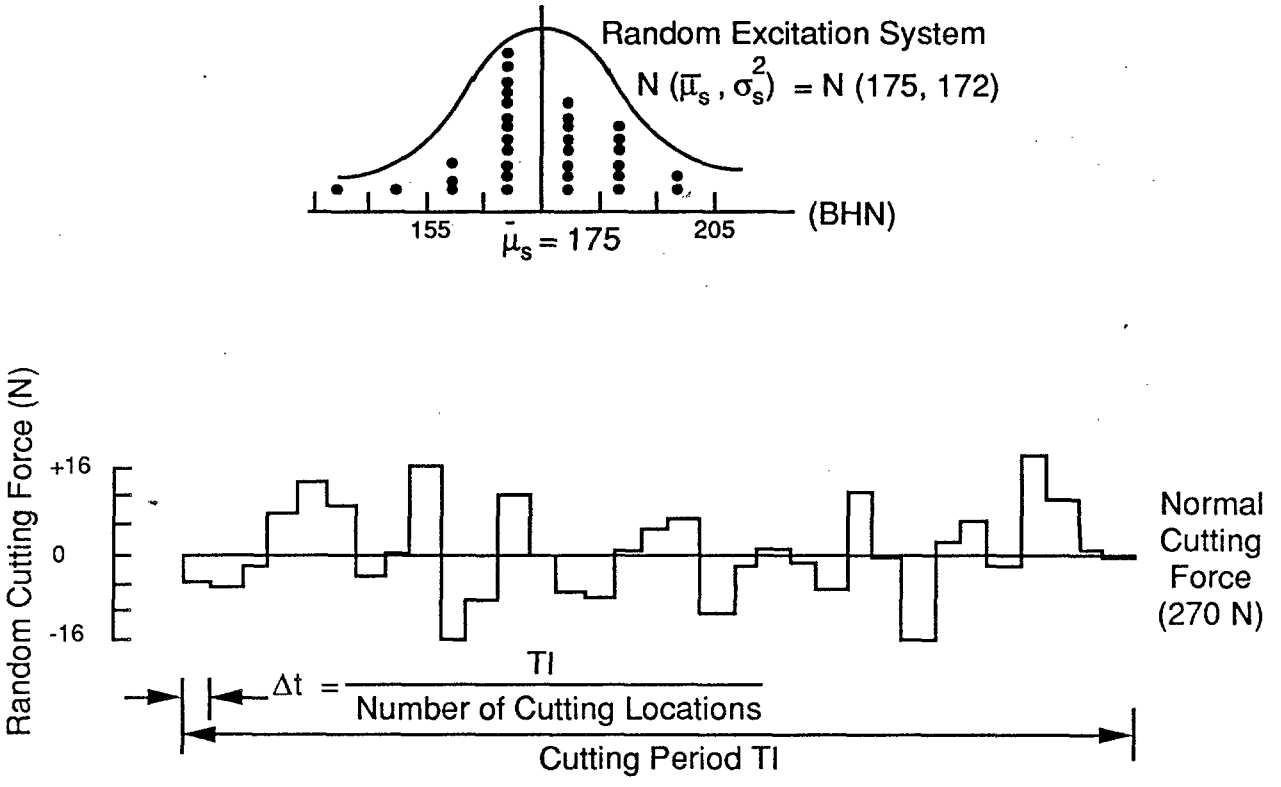

Fig. 4 Evaluation of the Random Excitation Force

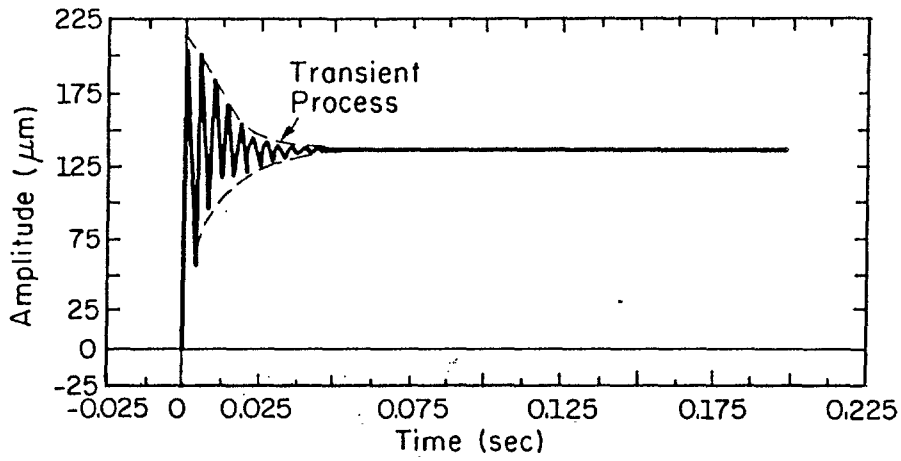

(a) Case 1: Continuous and without Random Excitation (N = 600 rpm)

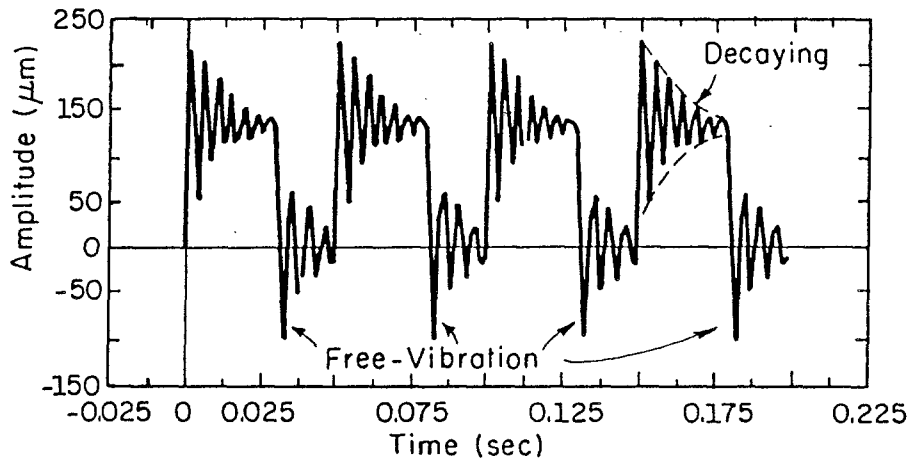

(b) Case 2: Discontinuous and without Random Excitation (N = 600 rpm)

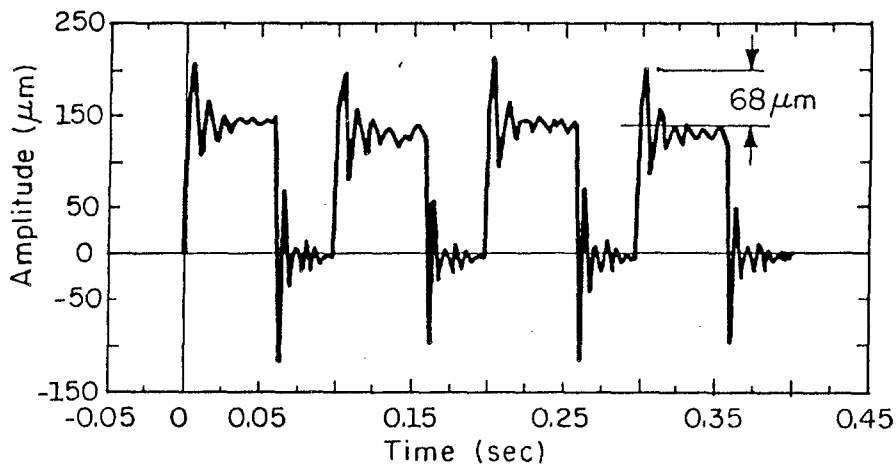

(c) Case 3: Discontinuous and with Random Excitation (N = 300 rpm)

Fig. 5 Simulation Results of the Six Case Studies

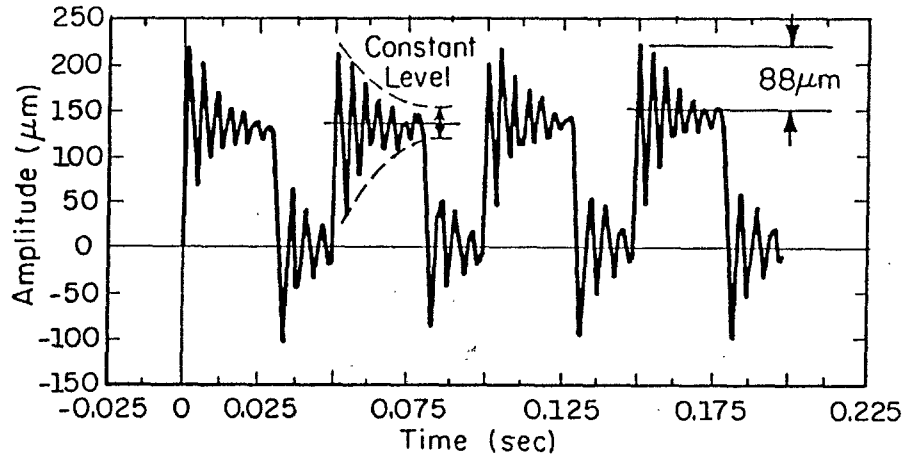

(d) Case 4: Discontinuous and with Random Excitation (N=600 rpm)

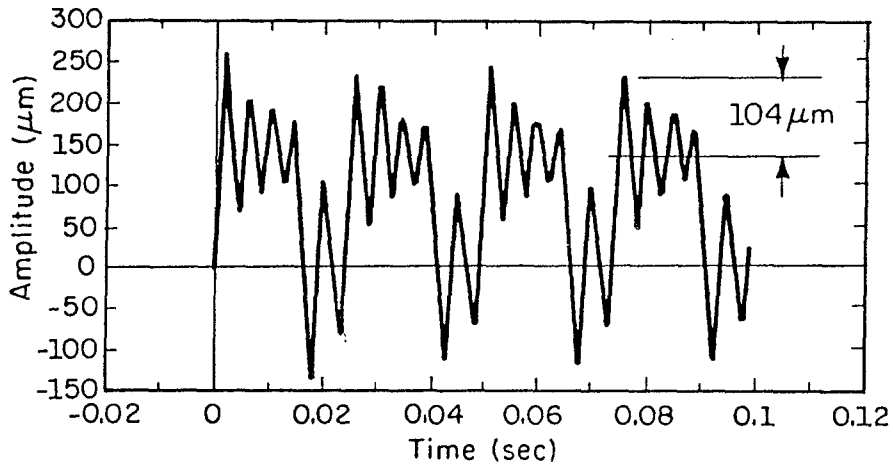

(e) Case 5: Discontinuous and with Random Excitation (N=1200 rpm)

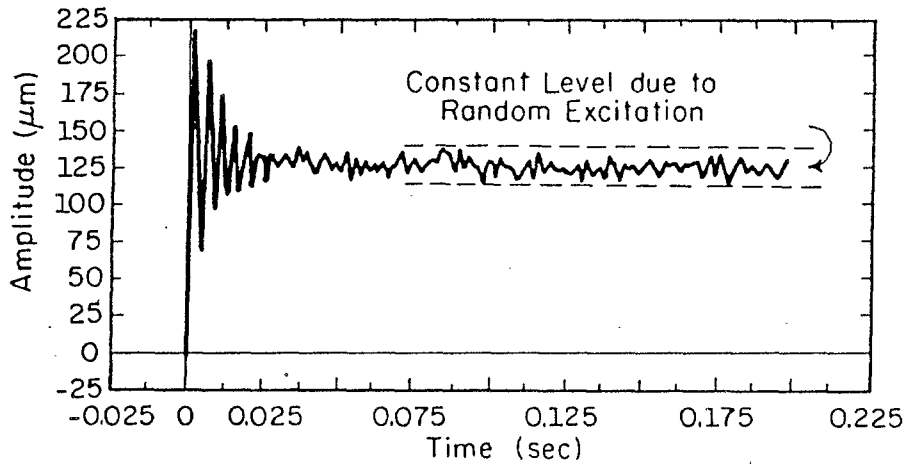

(f) Case 6: Continuous and with Random Excitation (N=600 rpm)

Fig. 5 Simulation Results of the Six Case Studies (Continued)

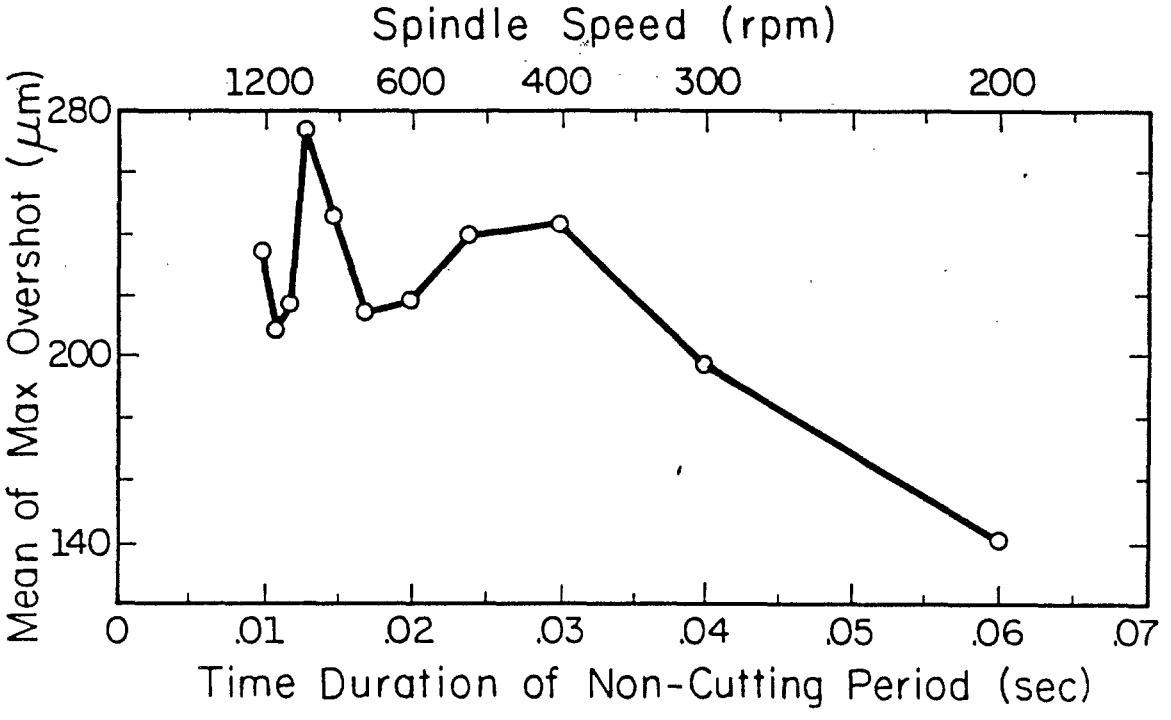

Fig. 6 Relation between the Mean of Maximum Overshot and Spindle Speed

Table 1 Simulation Conditions Used in the Case Studies

Case		Case 1	Case 2	Case 3	Case 4	Case 5	Case 6
workpiece Geometry		continuous	discontinuous	discontinuous	discontinuous	discontinuous	continuous
Random Vibration		Not Considered	Not Considered	Considered	Considered	Considered	Considered
cutting parameters	Feed mm/rev	0.30	0.30	0.30	0.30	0.30	0.30
	depth of cut mm	0.45	0.45	0.45	0.45	0.45	0.45
	spindle speed rpm	600	600	600	600	1200	600

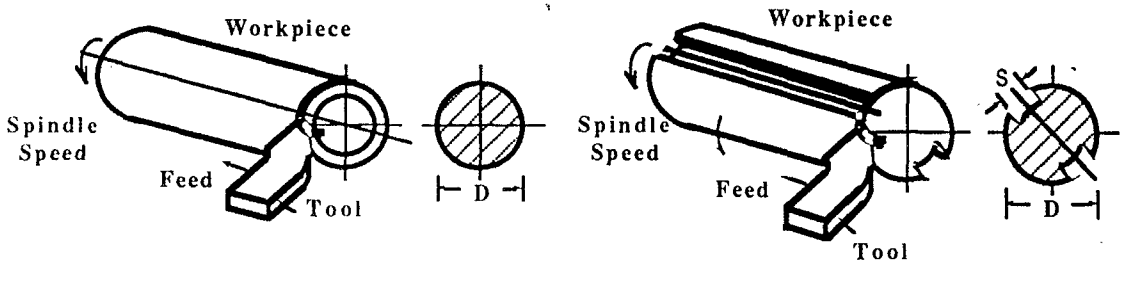

Diameter: 100 mm
Width of Slot: 60 mm

Table 2 Calculation of the Mean of Maximum Overshoot as a Function of the Spindle Speed

Spindle Speed (rpm)		200	300	400	500	600	700	800	900	1000	1100	1200
Time Duration of Non-Cutting Period (sec)		.060	.040	.030	.024	.020	.017	.015	.013	.012	.011	.010
Maximum Overshot Measured in Individual Cutting Periods (μm)	1	147	207	247	245	216	223	249	253	245	247	262
	2	146	192	229	226	203	204	237	272	201	194	232
	3	143	210	219	217	213	221	259	292	236	217	246
	4	140	199	239	239	210	213	243	278	209	199	229
	5	134	197	250	249	203	206	237	269	208	196	222
	6	149	194	243	240	220	205	237	266	215	213	234
	7	142	194	258	254	233	206	233	266	205	199	216
	8	145	204	263	260	238	224	247	276	212	196	227
	9	138	222	258	254	235	234	275	294	235	223	242
	10	137	163	225	224	208	202	243	274	208	200	232
Mean		142	198	243	240	218	214	246	274	217	208	234
Standard Deviation		4.57	14.6	14.2	13.7	12.5	10.4	12.0	11.6	14.6	16.0	12.4

* The tool dynamic equibrium position is at 130 μm from its static equilibrium position, which is set at zero.

Table 3 Decomposition of the Tool Vibration during the Cutting Period

Spindle Speed = 600 rpm					Spindle Speed = 600 rpm				
t	$y_1(t)$	$y_2(t)$	$y_3(t)$	$y(t)$	t	$y_1(t)$	$y_2(t)$	$y_3(t)$	$y(t)$
0.0000	0.00	0.00	-10.78	-10.78	0.00000	0.00	0.00	22.23	22.23
0.0015	210.22	8.03	4.99	223.24	0.00075	86.07	39.66	10.56	136.29
0.0030	158.29	-8.19	2.90	153.00	0.00015	210.22	33.21	-10.29	233.14
0.0045	55.52	2.41	-6.65	51.27	0.00225	240.11	-6.32	-17.71	216.09
0.0060	198.81	3.61	4.64	207.07	0.00300	158.29	-33.88	-5.97	118.44
0.0075	128.79	-5.47	2.20	123.52	0.00375	64.04	-22.93	10.24	51.34
0.0090	94.06	2.90	-3.64	93.32	0.00450	55.52	9.95	13.72	79.19
0.0105	181.36	1.09	3.56	186.02	0.00525	129.51	28.07	2.68	160.26
0.0120	118.04	-3.26	-0.94	113.84	0.00600	198.81	14.95	-9.56	204.20
0.0135	117.95	2.52	-1.68	118.79	0.00675	193.17	-11.64	-10.31	171.21
0.0150	164.96	-0.15	2.41	167.21	0.00750	128.79	-22.62	-0.41	105.77
0.0165	117.08	-1.71	-1.21	114.15	0.00825	79.74	-8.92	8.54	79.35
0.0180	131.09	1.86	-0.55	132.40	0.00900	94.06	12.00	7.50	113.55
0.0195	152.26	-0.63	1.46	153.09	0.00975	148.28	17.72	-1.07	164.94
0.0210	120.29	-0.74	-1.08	118.47	0.01050	181.36	4.52	-7.35	178.53
0.0225	137.22	1.22	0.02	138.46	0.01125	162.40	-11.47	-5.24	145.69
0.0240	143.64	-0.69	0.78	143.72	0.01200	118.04	-13.50	1.94	106.49
0.0255	124.55	-1.19	-0.81	123.54	0.01275	97.22	-1.43	6.13	101.92
0.0270	139.26	0.71	0.25	140.22	0.01350	117.95	10.42	3.47	131.83
0.0285	138.40	-0.58	0.25	138.16	0.01425	153.24	9.96	-2.37	160.82
0.0300	128.38	0.07	-0.54	127.91	0.01500	164.95	-0.63	-4.97	159.35
Maximum Variation Range (μm)	185	16	12		Maximum Variation Range (μm)	185	74	28	
Percentage	85%	8%	7%		Percentage	64%	26%	10%	